Enhanced Anharmonicity on Cu(110)

Liqiu Yang and Talat S. Rahman
Department of Physics, Cardwell Hall, Kansas State University, Manhattan, Kansas 66506

(Received 10 July 1991)

We report a temperature-dependent study of the vibrations and the structure of Cu(110) using molecular-dynamics codes based on potentials obtained from the embedded-atom method. The calculated linewidths and frequencies of the surface phonons and resonances and the mean-square vibrational amplitudes of the atoms indicate a sharp rise in surface anharmonic vibrations at about 600 K. Additionally, vacancies and adatoms begin to appear in the simulations of Cu(110) around 900 K. Comparison is made with experimental data and simulations of Cu(100).

PACS numbers: 68.35.Ja, 63.20.Dj, 68.35.Bs

In a theoretical framework, it is convenient to model a solid with only harmonic vibrations about equilibrium positions. In reality, such an approximation holds only at very low temperatures. Anharmonic vibrations are needed to account for phenomena, such as thermal expansion and finite thermal conductivity. At the more microscopic level too, anharmonic vibrations of a solid have been held accountable for properties like structural phase transitions, broadening of spectral linewidths with increasing temperature, and asymmetry in the radial distribution function of atoms. The effects of anharmonicity on the bulk microscopic properties of a solid have been studied theoretically using perturbative schemes including the quasiharmonic approximation [1].

With increasing evidence that the atoms in the surface layers experience enhanced anharmonic vibrations, in comparison with those in the bulk, the issue of surface anharmonicity has come to the forefront in surface studies. Several theoretical calculations based on perturbative schemes have already predicted quantitatively an increment in surface anharmonicity [2,3]. Subsequent observations on several metal surfaces, like the enlarged thermal expansion of Pb(110) [4] and the striking thermal attenuation of the diffracted beam (electron, He atom, x ray, or ion as the case may be) intensity for Al(110) [5], Cu(100) [6], Cu(110) [7-12], Ni(100) [13], and Ni(110) [14], have been cited as evidence for enhanced surface anharmonicity. For Cu(110) alternative explanations like the influence of thermal disorder [8,10] and surface roughening [9] have also been offered. Similarly, electron-energy-loss measurements of the surface-phonon frequency shift and linewidth broadening for Cu(110) have been proposed to be a direct reflection of the increased anharmonicity of surface vibrations [15]. Several years ago, angle-resolved photoemission studies on Cu(110) [16] had also pointed towards large anharmonic vibrations of the surface atoms, although the contribution of surface disorder to the results could not be ruled out. The debate on the importance of anharmonicity and/or disorder to the thermal attenuation of the diffracted beam intensities on Cu(110) has continued to be a lively one.

The work in this Letter has been inspired by the above findings and made possible by the availability of realistic interaction potentials. We present here molecular-dynamics (MD) simulations of the Cu(110) surface, for a range of surface temperatures, based on interatomic potentials from the embedded-atom method [17]. From the temporal development of the atomic positions and velocities the characteristics of the surface vibrational modes and of the structural order of this system are explored with three objectives. We show that the model potential produces reasonable agreement with the experimental data [15] on the surface-phonon linewidths and energy shifts and also with the observations on the temperature dependence of the mean-square vibrational amplitudes of the surface atoms [12]. Second, we present comparative results for the mean-square vibrational amplitudes in the bulk and in the surface, calculated without the limitations of perturbative methods for treating anharmonic terms in the potential. Finally, we compare the structure and the dynamics of Cu(110) with Cu(100) to find interesting differences in the structural order around 900 K. We argue that all our results point to enhanced surface anharmonicity as the leading effect on Cu(110), and not thermal disorder or roughening, between 600 and 850 K.

We have chosen the embedded-atom method (EAM) because of its feasibility, many-body nature, and physical picture of metallic bonding. The method is empirical in nature because of the assumptions [17] about the electronic charge densities and the fitting [17,18] of the potential to a large array of experimentally observed bulk quantities like lattice constant, elastic constants, cohesive energy, and vacancy formation energy. So far, for our purposes, the method has been successful in predicting quantities like the bulk and surface phonons [19] in several metals, surface relaxation [18], and reconstruction [20]. Our recent work [21] has further demonstrated that this model potential reproduces all the surface phonons and resonances in agreement with lattice-dynamical results based on force constants from *ab initio* calculations [22].

The details of the embedded-atom method and the procedures to obtain the numerical forms of the interatomic potential can be found elsewhere [17,18]. The essential elements of the simulational technique and the evaluation

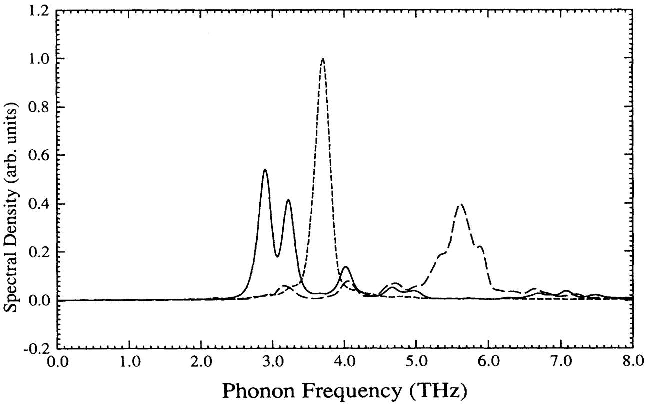

FIG. 1. Surface-phonon spectral densities for Cu(110) at 300 K at $\bar{X}$. The solid, long-dashed, and short-dashed lines represent the shear-vertical, longitudinal, and shear-horizontal components, respectively.

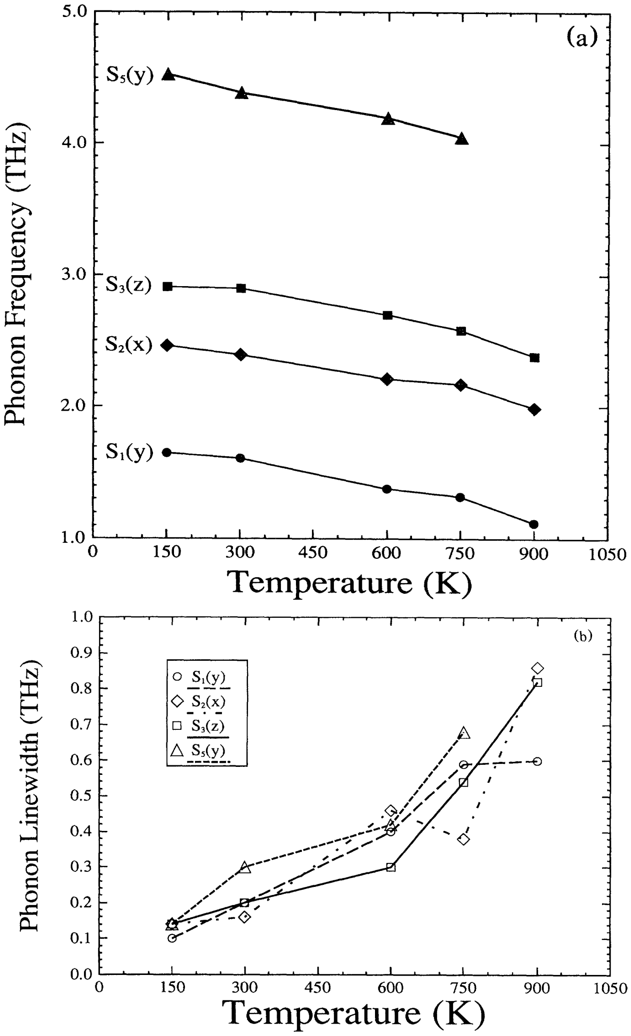

FIG. 2. Temperature dependence of surface phonons for Cu(110) at $\bar{Y}$. (a) The phonon frequencies; (b) the phonon linewidths. Here x, y, and z represent, respectively, the directions along the rows, across the rows, and normal to the surface.

of the phonon spectral densities and the vibrational amplitudes of the atoms may be found in Ref. [21]. Below is a short sketch of the MD simulation procedure.

Very briefly, the Newtonian equations of motion for atoms interacting via EAM potentials are solved numerically using the six-value Gear predictor-corrector algorithm with a time step of 1 fsec. For each temperature, first a zero-pressure bulk simulation is performed to obtain the equilibrium lattice constant. Next, to simulate the (110) surface, a ten-layer slab with 140 atoms per layer, arranged in the perfect lattice position, is used as the initial configuration. A 10-psec constant-temperature equilibration run is made, followed by a 50-psec constant-energy simulation at the specific temperature. The time evolution profile of the system collected in the long 50-psec run, essential to yield good statistics for calculations of the phonon spectral densities, is later used to evaluate the thermal averages of appropriate quantities.

The phonon spectral densities at 300 K for the first-layer atoms at the $\bar{X}$ point in the two-dimensional Brillouin zone are shown in Fig. 1. They have been evaluated from the Fourier transform of the layer-averaged velocity-velocity autocorrelation function [21,23]. The features in Fig. 1, in good agreement with the He scattering data [24], display the vertically polarized mode S_1 at 2.93 THz, the longitudinal mode MS_0 at 3.15 THz, the shear-horizontal "odd" mode S_2 at 3.77 THz, and the longitudinal "gap" mode S_7 at 5.6 THz. Part of the linewidth seen in Fig. 1 results from anharmonic effects and part from the Gaussian function employed to convolute the raw spectrum. The extra feature at 3.27 THz is an artifact arising from the standing mode of a finite (ten-layer) slab.

To make contact with experimental data [15], we plot in Fig. 2 the variations in the frequencies and linewidths of the surface phonons and resonances at zone boundary $\bar{Y}$. So far only the vertically polarized S_3 mode has been observed experimentally [15,24], at 300 K, with a frequency of about 2.9 THz [as in Fig. 2(a)]. The dispersion of the S_1 mode in the He scattering data suggests its frequency (it was observed up to $0.8\bar{Y}$) to be about 1.6 THz at $\bar{Y}$, in excellent agreement with our result. It will be very rewarding to observe this mode as a function of surface temperature since it undergoes a large softening [see Fig. 2(a)]. Another interesting temperature dependence is that of the gap mode S_5 which merges with the bulk band and hence broadens considerably around 750 K. Finally, the downward shift of 0.2 THz in the frequency of S_3 from 150 to 600 K compares well with the electron-energy-loss data [15]. No further data at higher temperatures on this mode are as yet available.

The variation of the surface-phonon linewidth with temperature, in Fig. 2(b), is very intriguing. The linear dependence of the width for high surface temperatures, as

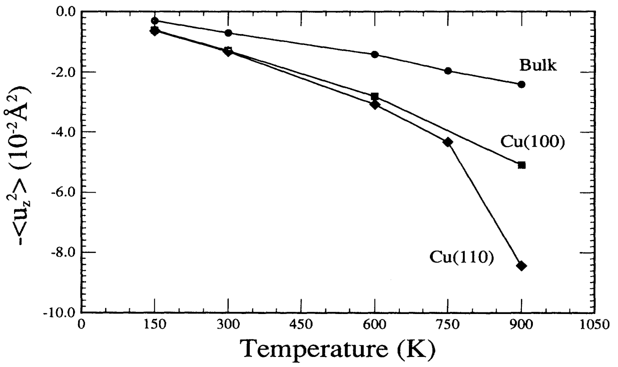

FIG. 3. Temperature dependence of the (vertical) mean-square displacements of Cu surface and bulk atoms.

found in perturbative calculations [25], holds for some temperature ranges, but overall the dependence is more complex. Here again data available for the S_3 mode from 150 to 553 K compare qualitatively with the observations in the figure. The actual magnitude of the broadening (0.16 THz) in this temperature range is about one-half of that reported in the data [15].

The slope of the curves in Fig. 2(b) has already given us an inkling of a peculiarity in the characteristic of the vibrational modes around 600 K. If we use the S_3 mode as our guide, there appears to be a large enhancement in the anharmonicity at 600 K. This conclusion is further strengthened from the plots of the mean-square vibrational amplitudes of the atoms in Fig. 3. The mean-square vibrational amplitude of the surface atoms is twice as large as that of the bulk atoms at low temperatures, but the deviation from the bulk value increases with increasing temperature, modestly until about 600 K, more substantially until 750 K, and then dramatically. The slope of the curve for the bulk atoms also registers an increment at 600 K but the effect is not as sharp as that for Cu(110). The mean-square vibrational amplitudes of Cu(100) top-layer atoms also display a sudden shift at 600 K but more modest than that for Cu(110). The trends in the figure for both surfaces have an amazing resemblance to the experimental data on the thermal attenuation of the He atom [7,11] and the low-energy electron [12] diffracted beam intensities. In fact, the actual numbers for the mean-square vibrational amplitudes on these surfaces extracted from the experimental data on intensities compare favorably with our calculations. Such a sharp enhancement in the vibrational amplitude has also been observed with low-energy electron diffraction on Ni(100) [14] and Ni(110) [13].

The calculated values of the mean-square vibrational amplitudes showing the anisotropy in the three directions are displayed in Table I for the first- and second-layer Cu(110) and for the bulk atoms. The conspicuously large value of the second-layer vertical mean-square vibrational amplitude shown in Table I was also found in the computer simulations of Ni(110) [26] at 1250 K also using EAM potentials. A similar table for Cu(100) in Ref. [21] shows the values for the second-layer atoms to be systematically less than those for the first layer. Cu(100) surface atoms also exhibit much less of an in-plane and out-of-plane anisotropy in the vibrational amplitudes. These differences in the behavior of the surface and second-layer atoms in the two crystallographic orientations are eventually reflected in the propensity to create vacancies and adatoms, as we shall see.

Comparison of the results for the mean-square vibrational amplitudes with earlier calculations [2] shows that, for the bulk atoms, our values are in reasonable agreement at 150 K with their value, 0.225×10^{-2} Å^2, considering our statistical error of $\pm0.05\times10^{-2}$ Å^2 at this temperature. However, at 300 and 600 K our values are larger than those in Ref. [2] by a factor of 1.75. We also do not find the out-of-plane vibrational amplitude to be larger than the in-plane ones as predicted in earlier works [2,27]. On the contrary, the in-plane (across the rows) vibration dominates for Cu(110).

It has been argued that apart from anharmonic effects, defects and disorder at the surface also help attenuate the intensity of diffracted beams at higher temperatures [8]. We have monitored the presence of vacancies and adatoms on the two Cu surfaces to find that up to 900 K the Cu(100) surface maintains its order, while beginning around 900 K Cu(110) starts to develop vacancies and adatoms, as seen in Fig. 4. Thus, Cu(100) does not disorder and Cu(110) does, but in our simulations this happens at 900 K and not 600 K, the temperature at which there is an onset of enhancement in the vibrational ampli-

TABLE I. Mean-square vibrational amplitude of atoms on the (110) surface and in the bulk of Cu (in units of 10^{-2} Å^2), with x and y representing the directions along and across the rows, respectively.

Temperature (K)	$\langle u_{1\perp}^2 \rangle$	$\langle u_{1x}^2 \rangle$	$\langle u_{1y}^2 \rangle$	$\langle u_{2\perp}^2 \rangle$	$\langle u_{2x}^2 \rangle$	$\langle u_{2y}^2 \rangle$	$\langle u_{\text{bulk}}^2 \rangle$
150	0.63	0.53	0.88	0.69	0.38	0.47	0.3
300	1.31	1.13	1.95	1.43	0.81	1.01	0.7
600	3.07	2.76	4.82	3.52	1.92	2.38	1.4
750	4.32	3.99	7.25	4.94	2.69	3.38	2.0
900	8.44	In-plane diffusion		7.05	4.05	5.47	2.4

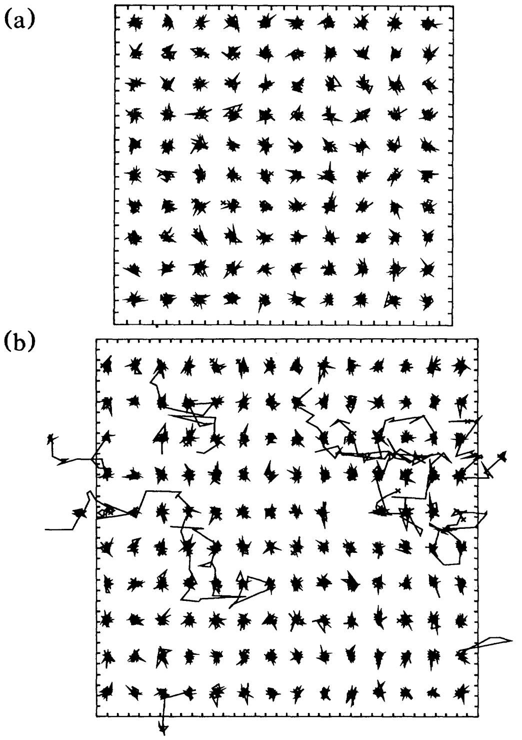

FIG. 4. Trajectories of Cu surface atoms at 900 K generated in molecular-dynamics simulations for a period of 50 ps. (a) Cu(100); (b) Cu(110).

tudes. The large value of 8.44×10^{-2} Å^2 for $\langle u_{\bar{1}1}^2\rangle$ for Cu(110) at 900 K is in this sense misleading since a contribution is coming from the diffusion of adatoms.

In conclusion, our molecular-dynamics simulations of Cu(110), Cu(100), and bulk Cu based on EAM potentials reproduce several of the experimentally observed features, all of which point to increased anharmonic vibrations of the surface atoms. But even more importantly, there is a very noticeable enhancement in the surface anharmonic behavior at 600 K. Furthermore, adatoms and vacancies are created around 900 K on Cu(110) while Cu(100) does not exhibit such disorder.

We thank Dr. Murray Daw for the EAM potential codes used in our simulations. This work was partially supported by the National Science Foundation under Grant No. DMR900015P. Supercomputer time was provided by the Pittsburgh Supercomputing Center.

---

[1] T. H. K. Baron and M. L. Klein, in *Dynamical Properties of Solids,* edited by G. K. Horton and A. A. Maradudin (Elsevier, New York, 1974), Vol. I, and references therein.

[2] S. K. S. Ma, F. W. deWette, and G. P. Aldredge, Surf. Sci. **78**, 598 (1978).

[3] C. S. Jayanthi, E. Tosatti, and L. Pietronero, Phys. Rev. B **31**, 3456 (1985); C. S. Jayanthi, E. Tosatti, and A. Fasolino, Phys. Rev. B **31**, 470 (1985).

[4] J. W. M. Frenken, F. Huusen, and J. F. van der Veen, Phys. Rev. Lett. **58**, 401 (1987).

[5] P. von Blanckenhagen, W. Schommers, and V. Voegele, J. Vac. Sci. Technol. A **5**, 649 (1987).

[6] G. Armand, D. Gorse, J. Lapujoulade, and J. R. Manson, Europhys. Lett. **3**, 1113 (1987).

[7] J. Lapujoulade, J. Perreau, and A. Kara, Surf. Sci. **129**, 59 (1983).

[8] D. Gorse and J. Lapujoulade, Surf. Sci. **162**, 847 (1985).

[9] S. G. J. Mochrie, Phys. Rev. Lett. **59**, 304 (1987).

[10] T. Fauster, R. Schneider, H. Dürr, G. Engelmann, and E. Taglauer, Surf. Sci. **189/190**, 610 (1987).

[11] P. Zeppenfeld, K. Kern, R. David, and G. Comsa, Phys. Rev. Lett. **62**, 63 (1989); G. Armand and P. Zeppenfeld, Phys. Rev. B **40**, 5936 (1989).

[12] S. Thevuthasan and W. N. Unertl, Appl. Phys. A **51**, 216 (1990); H. Dürr, R. Schneider, and Th. Fauster, Phys. Rev. B **43**, 12187 (1991).

[13] Y. Cao and E. H. Conrad, Phys. Rev. Lett. **65**, 2808 (1990).

[14] Y. Cao and E. H. Conrad, Phys. Rev. Lett. **64**, 447 (1990).

[15] A. P. Baddorf and E. W. Plummer, J. Electron Spectros. Relat. Phenom. **54/55**, 541 (1990); Phys. Rev. Lett. **66**, 2770 (1991).

[16] R. S. Williams, P. S. Wehner, J. Stöhr, and D. A. Shirley, Phys. Rev. Lett. **39**, 302 (1977).

[17] M. S. Daw and M. I. Baskes, Phys. Rev. B **29**, 6443 (1984).

[18] S. M. Foiles, M. I. Baskes, and M. S. Daw, Phys. Rev. B **33**, 7983 (1986).

[19] J. S. Nelson, M. S. Daw, and E. C. Sowa, Phys. Rev. B **40**, 1465 (1989); Phys. Rev. Lett. **61**, 1977 (1988); Luo Ningsheng, Xu Wenlan, and S. C. Chen, Solid State Commun. **67**, 837 (1988).

[20] S. M. Foiles, Surf. Sci. **191**, 329 (1987); M. S. Daw, Surf. Sci. **166**, L161 (1986).

[21] L. Yang, T. S. Rahman, and M. S. Daw (to be published).

[22] Y. Chen, S. Y. Tong, J.-S. Kim, L. L. Kesmodel, T. Rodach, K. P. Bohnen, and K. M. Ho (to be published).

[23] J. P. Hansen and M. L. Klein, Phys. Rev. B **13**, 878 (1976).

[24] P. Zeppenfeld, K. Kern, R. David, K. Kuhnke, and G. Comsa, Phys. Rev. B **38**, 12329 (1988).

[25] A. A. Maradudin and A. E. Fein, Phys. Rev. **128**, 2589 (1962).

[26] E. T. Chen, R. N. Barnett, and U. Landman, Phys. Rev. B **41**, 439 (1990).

[27] A. A. Maradudin and J. Melngailis, Phys. Rev. **133**, A1188 (1964); R. F. Wallis, in *The Structure and Chemistry of Solid Surfaces,* edited by G. A. Somorjai (Wiley, New York, 1967), Chap. 17.